

A Novel Biometric Personal Verification System Based on the Combination of Palmprints and Faces

Slobodan RIBARIĆ, Ivan FRATRIĆ, Kristina KIŠ

*Faculty of Electrical Engineering and Computing, University of Zagreb
Unska 3, 10000 Zagreb, Croatia
e-mail: slobodan.ribaric@fer.hr*

Received: February 2007

Abstract. This paper presents a bimodal biometric verification system based on the fusion of palmprint and face features at the matching-score level. The system combines a new approach to palmprint principal lines recognition based on hypotheses generation and evaluation and the well-known eigenfaces approach for face recognition. The experiments with different matching-score normalization techniques have been performed in order to improve the performance of the fusion at the matching-score level. A “chimerical” database consisting of 1488 palmprint and face image pairs of 241 persons was used in the system design (440 image pairs of 110 persons) and testing (1048 image pairs of 131 persons). The experimental results show that system performance is significantly improved over unimodal subsystems.

Key words: multimodal biometrics, verification, normalization, fusion, palmprint, face.

1. Introduction

Biometrics is an emerging technology that utilizes distinct behavioural or physiological characteristics in order to determine or verify the identity of an individual (Jain *et al.*, 1999a; Zhang, 2000). The physical characteristics used in biometric identification or verification systems are fingerprint (Jain *et al.*, 1999b), hand geometry (Kumar *et al.*, 2003a; Ribaric *et al.*, 2003), palmprint (Shu and Zhang, 1998; Zhang and Shu, 1999; Duta *et al.*, 2001; You *et al.*, 2002; Han *et al.*, 2003; Lu *et al.*, 2003; Wu *et al.*, 2003; Wu *et al.*, 2004; Zhang *et al.*, 2003), face (Turk and Pentland, 1991; Belhumeur *et al.*, 1997; Jain *et al.*, 1999b; Jonsson *et al.*, 1999; Kotropoulos *et al.*, 2000; Zhao *et al.*, 2000), iris (Zhang, 2000), retina and ear (Jain *et al.*, 1999a). The behavioural characteristics are signature, lip movement, speech, keystroke dynamics, gesture and gait (Jain *et al.*, 1999a; Zhang, 2000). Biometric systems that use a single trait are called unimodal systems, whereas those that integrate two or more traits are referred to as multimodal biometric systems. Although unimodal systems are usually more cost-efficient than multimodal systems, a single biometric trait might not be enough to authenticate a user, and so multimodal systems are being developed in order to provide acceptable performance, to increase the scalability and the reliability of decisions and to increase the system’s robustness to fraudulent technologies (Bolle *et al.*, 2004; Jain and Ross, 2004; Ross and Jain, 2003).

In this paper we describe a bimodal biometric verification system for physical or logical access control based on palmprint and facial features. Related work in the fields of palmprint and face-based authentication, as well as fusion at the different levels, is given in the following paragraphs.

The palm is the inner surface of the hand between the wrist and the fingers (Zhang and Shu, 1999). The palm area contains a large number of features that can be used as biometric features, such as principal lines, geometry, wrinkle, delta point, minutiae and datum point features. Shu and Zhang (1998) used both geometrical features of the palmprint and points along the principal lines of the palmprint to distinguish one person from among others. Zhang and Shu (1999) located datum points using a directional projection algorithm, and afterwards line-feature extraction and matching were applied in order to detect whether two palmprints belong to the same palm. Duta *et al.* (2001) extracted a number of feature points from the prominent palm lines; the decision as to whether two hands belong to the same person was based on the matching score between the corresponding sets of feature points for the two palmprints. You *et al.* (2002) first used global texture energy to select a small set of similar candidates from the database, and then used point-based matching to make the final decision. Han *et al.* (2003) used Sobel and morphological operations to extract features from the palm area. Wu *et al.* (2003) used a set of directional line detectors to detect the principal lines of the palm, which are then used to classify palms into one of six categories according to the number of principal lines and the number of their intersections. Ribaric *et al.* (2003) and Kumar *et al.* (2003) combined line-like features of the palm and hand geometry into a multimodal biometric system for user authentication. In addition to the approaches based on these palmprint features, other approaches have been developed for palmprint-based biometric systems as well, such as eigenpalms (Lu *et al.*, 2003;), fisherpalm (Wu *et al.*, 2003), Fourier transform (Li *et al.*, 2002) and 2D Gabor phase encoding (Zhang *et al.*, 2003).

From the numerous methods developed for the purpose of face recognition (Zhao *et al.*, 2000), the use of eigenfaces (Turk and Pentland, 1991) is one of the most popular. Turk and Pentland (1991) first used eigenfaces by applying the method known as the Karhunen–Loeve (K–L) transform or PCA (Principal Component Analysis) to a set of facial images. The method functions by projecting the facial images onto a feature space that spans the significant variations among the known facial images. The feature-space basis vectors are called eigenfaces because they are eigenvectors of the covariance matrix of the known facial images. The facial features are obtained by projecting the facial image into the obtained feature space, and these features do not necessarily correspond to our intuitive notion of the facial features. Some other recent face recognition approaches include fisherfaces (Belhumeur *et al.*, 1997), support vector machines (Jonsson *et al.*, 1999) and elastic graph matching (Kotropoulos *et al.*, 2000).

A multimodal biometric system requires an integration scheme to fuse the information obtained from the individual modalities. Various levels of fusion are possible (Kittler and Alkoot, 2003; Ross and Jain, 2003):

- i) fusion at the feature-extraction level, where the feature vector is obtained using data from multiple sensors;

- ii) fusion at the matching-score level, where the matching scores obtained from multiple matchers are combined;
- iii) fusion at the decision level, where the accept/reject decisions of multiple systems are consolidated.

Multimodal biometric systems based on palmprint and hand-geometry features (Kumar *et al.*, 2003; Ribaric *et al.*, 2003), face, fingerprint and hand-geometry features (Ross and Jain, 2003; Jain and Ross, 2004) and fingerprint, face and speech (Jain *et al.*, 1999c) have been described.

Kumar and Zhang (2003) describe an integration of already described approaches for palmprint (Kumar *et al.*, 2003) and face (Turk and Pentland, 1991) recognition. The proposed method of fusion uses neural network to integrate individual matching scores and generate a combined decision score. The system was tested on the database consisting of only 40 subjects (10 images per subject). The performance scores expressed as the minimum total error rate (mTER) are: 13.04% for face, 6.90% for palmprint and 1.53% for fusion at decision level.

Early version of our system based on fusion of palmprint and face features and results of preliminary experiments has been described in (Ribaric *et al.*, 2005).

The rest of this paper is organized as follows: In Section 2 the bimodal biometric system is described in detail. The experimental results obtained by our system are reported in Section 3. The conclusion and future work are presented in Section 4.

2. A Bimodal Biometric System

2.1. System Overview

Fig. 1. shows the block-diagram of the proposed bimodal biometric verification system.

The system's input is provided as a pair of images: a palmar image, at the resolution of 180 dpi and a frontal facial image (720×576 pixels). The processing of these images, up until fusion, is carried out separately in the palmprint recognition and the face recognition subsystems. In the first phase of the palmprint recognition process the area

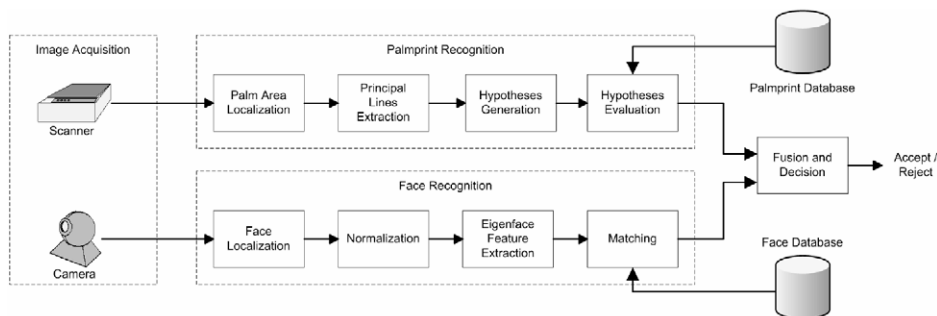


Fig. 1. Block-diagram of the proposed bimodal biometric verification system.

of the palm is located on the basis of the hand contour and the stable points. In the second phase the principal lines of the palm are extracted using line-detection masks (Zhang and Shu, 1999) and a line-following algorithm (Maio and Maltoni, 1999). The matching of palmprint templates is based on hypotheses generation and their evaluation similar to the HYPER (Ayache and Faugeras, 1986) method, originally used for recognition and positioning of 2-D objects.

The process of face recognition consists of four phases: face localization based on the Hough method (Hough, 1962) normalization, including geometry and lighting normalization; feature extraction using eigenfaces; and finally, matching of the live-template to the templates stored in the face database.

Matching scores from both recognition modules are combined into a unique matching score using fusion at the matching-score level. Based on this unique matching score, a decision about whether to accept or reject a user is made.

2.2. Palmprint Recognition

In order to localize the palm area, the first step is to preprocess the palmar images; this involves Gaussian smoothing and contrast enhancement. Due to the regular and controllable illumination conditions simple global thresholding provides satisfactory segmentation. After that, a contour-following algorithm is used to extract the hand contour. The two stable points on the hand contour are found (Ribaric *et al.*, 2003): (i) The gap between the little finger and the ring finger, and (ii) The gap between the index finger and

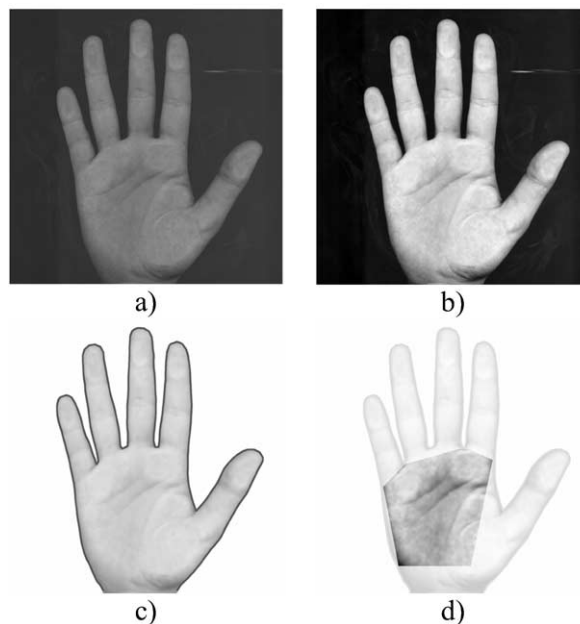


Fig. 2. An example of palm-area localization: a) original image, b) image after preprocessing, c) extracted hand contour projected on the grey-scale image, d) localized area of the palm.

the middle finger. Based on the stable points on the contour, the palm area on the preprocessed grey-scale image, which is represented by a hexagonal area, is determined. Fig. 2 shows the phases of palm-area localization.

Process of principle lines and other prominent palm lines extraction begins with convolving the grey-scale palmprint area by four line detection masks (Zhang and Shu, 1999). Fig. 3 presents the results of applying the line detection masks to the palm area.

After applying the modified line-following algorithm, based on the work of Maio and Maltoni (Maio and Maltoni, 1999), a set of lines is obtained. Examples of the palm-line extraction are presented in Fig. 4.

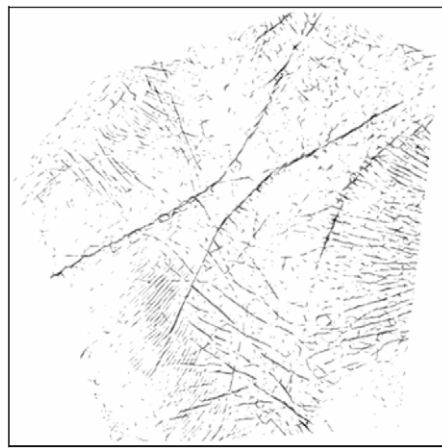


Fig. 3. The results of applying the line-detection masks to the palm area.

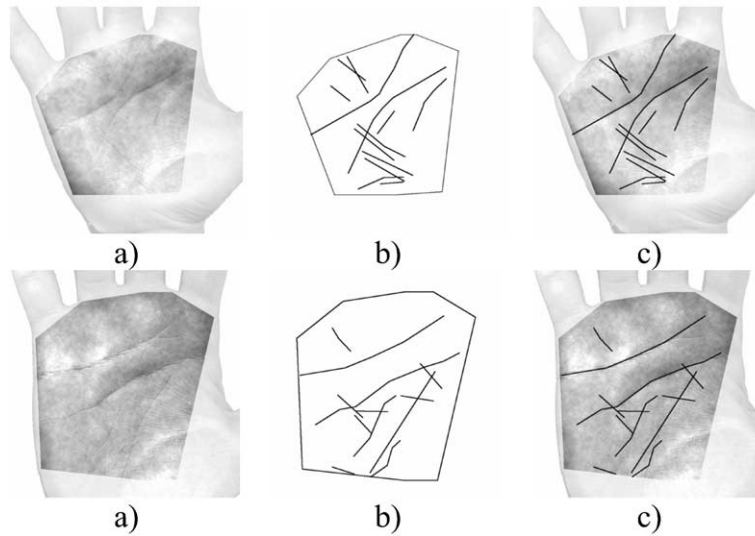


Fig. 4. Examples of palm-line extraction: a) palm area, b) extracted lines, c) overlapped image a) and b).

The extracted lines are described in a hand-coordinate system that is based on the above two stable points. This makes them invariant to hand translation and rotation. The palm lines are represented by means of the line-segment sequence, where each segment is described by a four-tuple (x, y, l, α) , where x and y are the coordinates of the segment midpoint, l is the length of the segment and α is the segment orientation.

The obtained line set contains the most prominent palm lines. The number of lines can vary depending on the palmprint texture and wrinkles. Typically, the number of lines extracted from a palm region is between 15 and 20, with 1 to 5 line segments per line.

The matching of the live-template and the template from the database is based on hypotheses generation and their evaluation, using the adapted HYPER method (Ayache and Faugeras, 1986).

The hypotheses-generation stage consists of finding the corresponding line pairs (one from each template). These pairs are then evaluated, all the line segments belonging to the two corresponding lines are compared and each segment's matching coefficient is updated. After all the hypotheses have been evaluated, the final palmprint-similarity measure is computed.

Generating Hypotheses

Since the obtained palm lines are invariant to hand translation and rotation, the two lines (one from the live-template and one from the palmprint database-template) can correspond to each other only if they have a similar position and orientation. Every palm line from the live-template is compared to every palm line from the database-template and a decision is made about whether to add this pair to the hypothesis collection.

Let p be the virtual line that connects the midpoints of the first and the last segment of the i th palm line $L_{i,LT}$ from the live-template, and let p' be the virtual line that connects the midpoints of the first and the last segments of the j th palm line $L_{j,DB}$ from the database-template. The palm lines are compared in the following way:

1. If the absolute angular difference between the lines p and p' is greater than α_{gen_max} , then the palm lines are dissimilar and no further comparison is necessary. Otherwise, Step 2 is performed. In this application the value of α_{gen_max} is set to $\pi/5$, based on the training set of the palmprint database.
2. The average Euclidian distance d_{gen_12} between the line p' and the segment midpoints of the palm line from the live-template is calculated:

$$d_{gen_12} = \frac{1}{n_{i,LT}} \sum_{k=1}^{n_{i,LT}} d(s_{1k}, p'), \quad (1)$$

where $n_{i,LT}$ is the number of line segments in $L_{i,LT}$ and $s_{1k} = (x_k, y_k)$ is the midpoint of the k th segment belonging to the line $L_{i,LT}$.

The average distance between the line p and the segment midpoints of the palm line from the database-template is calculated in a similar manner:

$$d_{gen_21} = \frac{1}{n_{j,DB}} \sum_{k=1}^{n_{j,DB}} d(s_{2k}, p), \quad (2)$$

where $n_{j,DB}$ is the number of line segments in $L_{j,DB}$ and $s_{2k} = (x_k, y_k)$ is the midpoint of the k th segment belonging to the line $L_{j,DB}$. In general, $n_{i,LT} \neq n_{j,DB}$. The smaller of these distances is taken as a measure of the distance between the two palm lines: $d_{gen} = \min(d_{gen_12}, d_{gen_21})$. If d_{gen} is smaller than the threshold d_{gen_max} , then the pair of palm lines is added to the hypothesis collection HC ; otherwise the lines are considered to be dissimilar. The experimentally selected value for d_{gen_max} is 50 pixels (for the spatial resolution of 180 dots per inch).

Evaluating Hypotheses

The hypothesis collection consists of all the line pairs (one line from the live-template and one from the database-template) that satisfy the hypotheses generation conditions. The hypothesis collection is defined as $HC = \{(L_{i,LT}, L_{j,DB})\}$, $i \leq N_{LT}$ and $j \leq N_{DB}$, where N_{LT} is the number of lines in the live-template and N_{DB} is the number of lines in the database-template. In general $N_{LT} \neq N_{DB}$.

Evaluating a hypothesis $H = (L_{i,LT}, L_{j,DB})$, $H \in HC$ consists of comparing every line segment of $L_{i,LT}$ with every line segment of $L_{j,DB}$ and updating the matching measure for each line segment. For every line-segment pair (S_k, S_l) ; $S_k \in L_{i,LT}$, $S_l \in L_{j,DB}$ where $S_k = (x_k, y_k, l_k, \alpha_k)$ and $S_l = (x_l, y_l, l_l, \alpha_l)$, $k = 1, 2, \dots, n_{i,LT}$, $l = 1, 2, \dots, n_{j,DB}$, the following parameters are calculated:

1. The absolute angular difference $a = |\alpha_k - \alpha_l|$, where α_k and α_l are orientations of corresponding line segments;
2. The Euclidean distance d between the midpoints of the segments;
3. The Euclidean distance D_{kq} between the midpoint (x_k, y_k) and the virtual line q that segment S_l lies on is computed. Analogously, the distance D_{lr} between the midpoint (x_l, y_l) and the virtual line r that segment S_k lies on is computed. Parameter D is defined as the minimum of the two distances: $D = \min(D_{kq}, D_{lr})$.

Each parameter is upper-bounded by the values a_{max} , d_{max} and D_{max} , respectively. The dissimilarity measure, dm_{kl} , for the segment pair (S_k, S_l) is computed in the following way:

1. If $a > a_{max}$ or $d > d_{max}$ or $D > D_{max}$, then $dm_{kl} = 1$; the segments are entirely dissimilar.
2. Otherwise, set $dm_{kl} = w_1 \cdot a/a_{max} + w_2 \cdot D/D_{max} + w_3 \cdot d/d_{max}$.

The parameters w_1 , w_2 and w_3 represent the weights given to parameters a , D and d , respectively ($w_1 + w_2 + w_3 = 1$, $w_1 \geq 0$, $w_2 \geq 0$, $w_3 \geq 0$). The dissimilarity measure, dm_{kl} , is a number in the range $[0, 1]$, and has a lower value for more similar segments. The experimentally determined parameter values are $w_1 = 0.5$, $w_2 = 0.4$, $w_3 = 0.1$,

$a_{max} = \pi/18$, $D_{max} = 10$ pixels and $d_{max} = \max(l_k, l_l)$, where l_k and l_l represent the lengths of the segments S_k and S_l , respectively.

After computing the dissimilarity measure, the measures of matching m_k and m_l for segments S_k and S_l need to be updated. The measures of matching are updated using the following formulas:

$$m_k = m_k + (1 - dm_{kl}) \cdot \min(l_k, l_l), \quad (3)$$

$$m_l = m_l + (1 - dm_{kl}) \cdot \min(l_k, l_l). \quad (4)$$

More than one line segment from $L_{i,LT}$ or $L_{j,DB}$ can contribute to the matching measure of segments from $L_{j,DB}$ or $L_{i,LT}$, respectively. If a line L appears in more than one hypothesis, the matching measures of its line segments are accumulated.

The similarity measure, $Q_{A,B}$, of the palmprint template A and the palmprint template B is expressed in the range $[0, 1]$ and gives an indication of how fully template A is represented within template B . Two similarity measures, $Q_{LT,DB}$ and $Q_{DB,LT}$, are computed. The $Q_{LT,DB}$ is computed as the sum of matching measures of all segments in all lines in the live-template, normalized by the sum of their lengths. Analogously, the similarity measure $Q_{DB,LT}$ is computed (in general, $Q_{LT,DB} \neq Q_{DB,LT}$).

The final similarity measure Q , which determines how well the two samples match, is obtained in the following way: compute $|T_H - Q_{LT,DB}|$ and $|T_H - Q_{DB,LT}|$ and select Q for which the above absolute value is greater, where T_H is a threshold selected experimentally during the training phase ($T_H = 0.25$). Fig. 5 shows the similarity measure Q for several palmprint template pairs.

2.3. Face Recognition

Faces in images are localized using an approach that combines the Hough method (Hough, 1962) and skin-colour information (Jones and Rehg, 1999) for face localization (Pavesic *et al.*, 2004). The Hough method for ellipses is applied on multiple image scales to locate a number of candidates for a face in the image. In order to reduce the computational complexity, the sought ellipses have a fixed height/width ratio. After the candidates have been proposed, they are verified using skin-colour information and a heuristic approach based on a horizontal projection. When a face candidate is selected, the system proceeds by locating the eyes using a simple neural network. In Fig. 6 two examples of face localization are presented.

Since the K-L transform is used for matching, a normalization procedure is required. Face normalization consists of geometry normalization, background removal and lighting normalization. Geometry normalization involves image rotation, translation and the scaling of the images. The locations of the eyes obtained in the localization phase are used as the reference points in this step. The images of the faces are normalized to a fixed size of 64×64 pixels. The background is removed by leaving only the image elements inside the elliptical region in the normalized images and setting the rest to 0 (black). In the final normalization step, lighting normalization using histogram fitting is applied (Gonzales and Woods, 1993). In Fig. 7, several images after the normalization phase are shown.

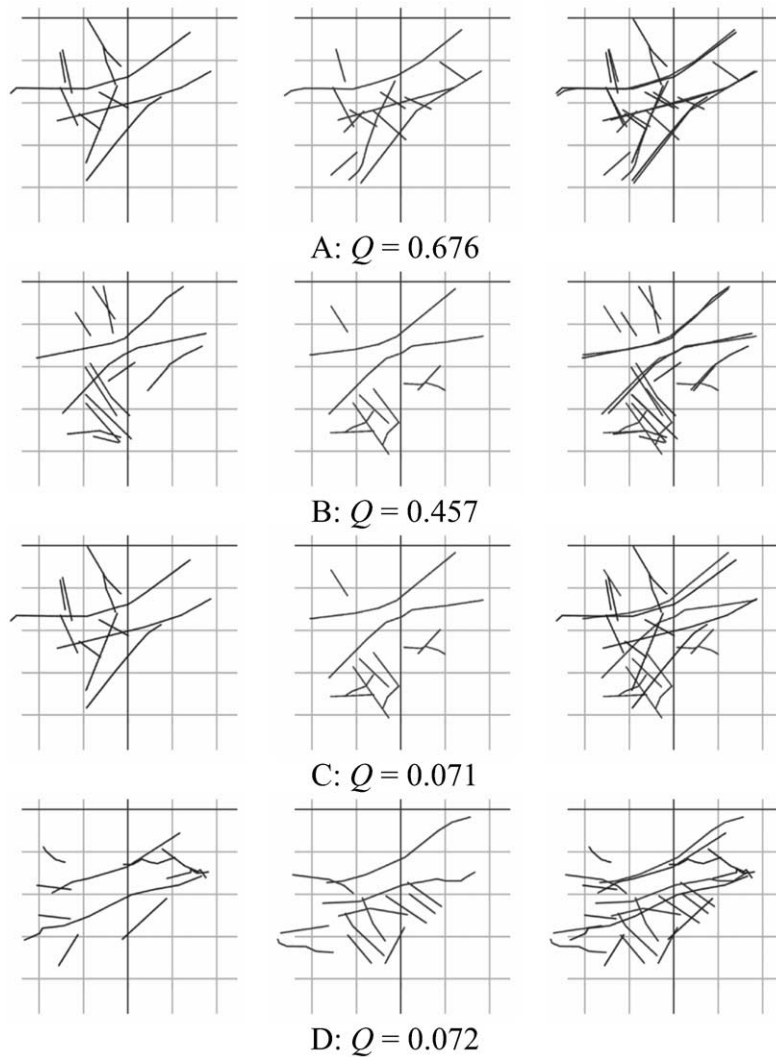


Fig. 5. Comparison of palmprint templates and similarity measure Q : A, B – comparison of palmprint templates of the same person; C, D – comparison of palmprint templates of different people. The first and the second columns represent the individual palmprint templates. The third column represents both templates in the same coordinate system.

The eigenfaces technique (Turk and Pentland, 1991), used in our system for feature extraction, is a widely used method for face recognition (Navarrete and Ruiz-Del-Solar, 2002). It is based on the K–L transform applied to a set of facial images. The K–L transform finds a subspace of the image space that the set of training images occupy. It has the property of being able to represent the images using the minimum number of samples (i.e., no other transform exists that can represent these images with the same number of

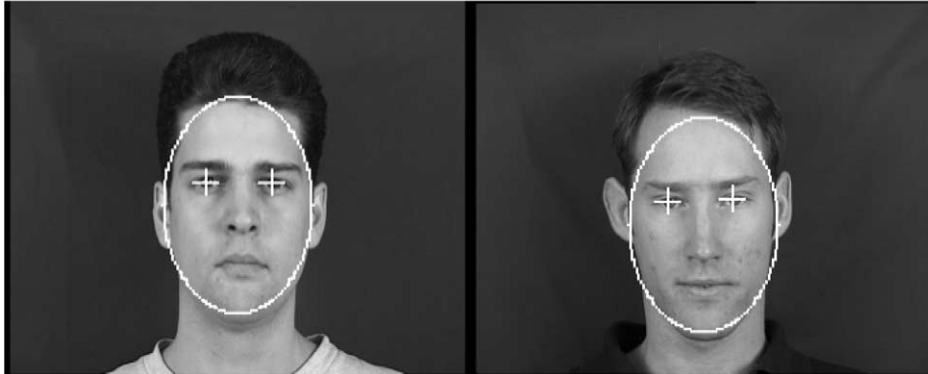


Fig. 6. Examples of face localization.



Fig. 7. Several faces after the normalization phase.

samples and has a smaller reconstruction error). Therefore, the K–L transform finds the optimal features for image representation, but not necessarily for optimal discrimination.

The basis vectors of the K–L transform are calculated by finding the largest m eigenvectors of the covariance matrix of the set of images. In the case of facial images, when representing these eigenvectors as images, they will resemble faces, and are called eigenfaces. The subspace these eigenvectors' span is called the face-space. Some of the eigenfaces obtained using the training database are presented in Fig. 8.

It is clear that the largest eigenvectors (those with the smallest ordinal numbers) look more like faces, while those with the largest ordinal numbers look more like noise. The largest eigenvectors carry the useful information (in the sense of image representation) and only they are used as the basis for the face-space, while the information carried by the smaller eigenvectors is lost in the process of encoding. Based on the preliminary recognition experiments on the training database, we chose $m = 111$ for the face-space dimensionality.

The feature vector from an unknown facial image can be obtained by projecting the image onto a face-space. In this process the image is represented as a linear combination of eigenfaces and the feature vector is made of weightings associated with each eigenface. The face template consists of this 111-component feature vector. The matching score between two face-feature vectors is calculated using the Euclidean distance in the matching phase.

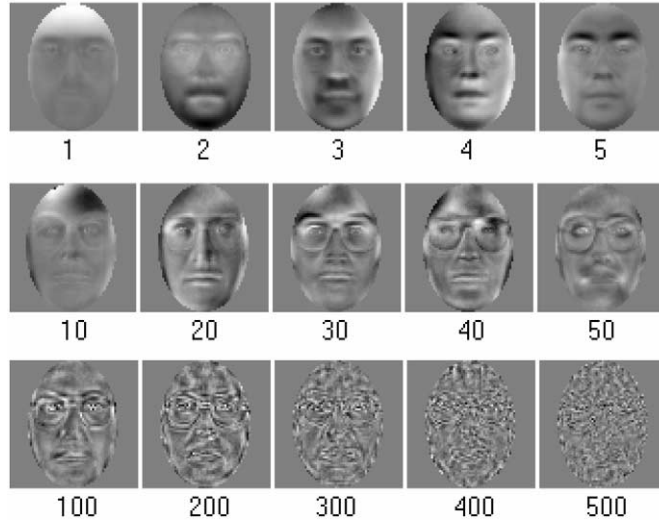


Fig. 8. Eigenfaces obtained on the training database with appropriate ordinal numbers.

2.4. Fusion and Decision

Fusion at the matching score level is the most common approach due to its simplicity and good performance (Jain *et al.*, 2005). Kittler and Alkoot (2003) have analytically shown that, for Gaussian error distributions, fusion based on sum always outperforms fusion based on vote. Ross and Jain (2003) have also experimentally shown that matching score sum fusion performs better than some other fusion methods such as decision trees and linear discriminant analysis.

In our bimodal biometric system the fusion is performed at the matching-score level.

When trying to verify the identity of an unknown sample we receive two sets of scores from the two independent matching modules:

- Palmprint similarity measures, denoted as Q in subsection 2.2, for notational convenience, in the remainder of the text will be denoted as similarity scores $s^P(\mathbf{P}_x, \mathbf{P}_j)$, where \mathbf{P}_x is the unknown palmprint-template, and \mathbf{P}_j , $j = 1, 2, \dots, n$ are palmprint-templates stored (enrolled) in the database under the identity the system is trying to verify.
- Euclidean distance scores will be denoted as $s^F(\mathbf{F}_x, \mathbf{F}_j)$, where \mathbf{F}_x is the unknown face-template, and \mathbf{F}_j , $j = 1, 2, \dots, n$ are the face-templates stored (enrolled) in the database under the identity the system is trying to verify.

In order to generate the unique matching score we need a way to combine individual matching scores from face- and palmprint-matching modules. Since the palmprint-matching scores and the face-matching scores are of the different type (i.e., distances and similarities) and come in different numerical ranges, normalization has to be performed before they are combined (Jain *et al.*, 2005).

We experimented with the heuristic normalization techniques (Ribaric and Fratric, 2006) (piecewise-linear, min-max, median-MAD, double-sigmoid, tanh, z-score) and Bayes-based normalization. The Bayes-based normalization provided the best system performance.

Bayes-based Normalization

The Bayes-based normalization was carried out by estimating the probability density of genuine scores by means of the Bayes formula:

$$P(\text{genuine}|s) = \frac{p(s|\text{genuine}) \cdot P(\text{genuine})}{p(s|\text{genuine}) \cdot P(\text{genuine}) + p(s|\text{impostor}) \cdot P(\text{impostor})}, \quad (5)$$

where s represents the raw score obtained directly from the matching module. However, prior probabilities of genuine users and impostors, $p(s|\text{genuine})$ and $p(s|\text{impostor})$, are generally not known, and they have to be estimated based on the scores obtained from the training data. We used Parzen window approach to estimate prior distributions (Duda *et al.*, 2001). Distributions for the palm scores obtained on our training data can be seen on Figs. 9 (a) and 9 (b) for the palmprint and face scores, respectively. Based on the

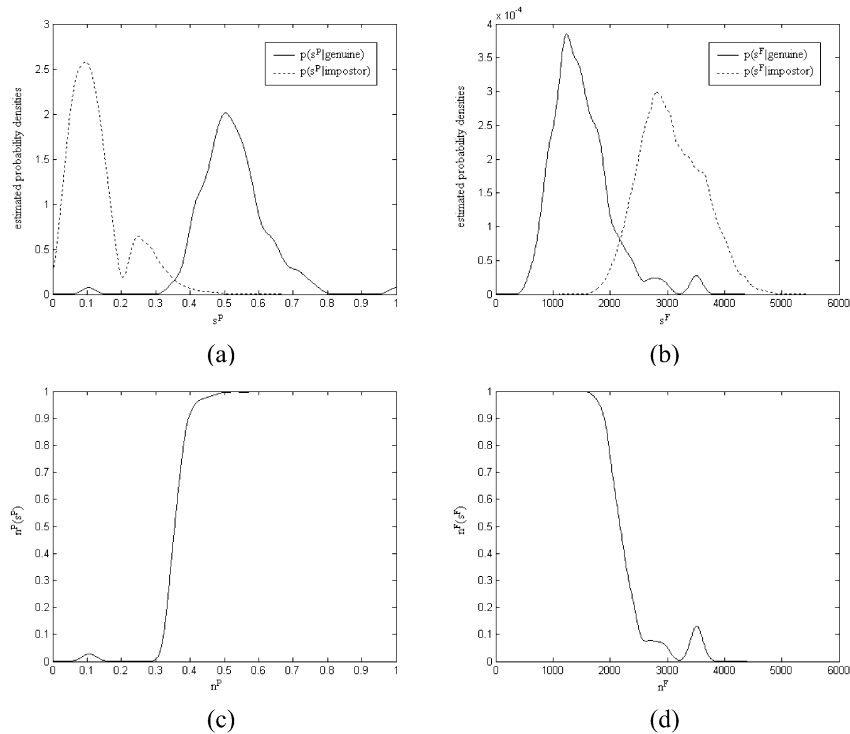


Fig. 9. (a) Estimated genuine and impostor palmprint score distributions, (b) Estimated genuine and impostor face score distributions, (c) Palmprint score normalization function, (d) Face score normalization function.

Byes formula (5) we obtain the normalization functions for palmprint and face matching scores, $n^P(s^P)$ and $n^F(s^F)$, as

$$n^P(s^P) = P(\text{genuine}|s^P), \quad (6a)$$

$$n^F(s^F) = P(\text{genuine}|s^F). \quad (6b)$$

The obtained normalization functions for face and palmprint scores can be seen on Figs. 9 (c) and 9 (d), respectively.

The maximum similarity measure of $s^P(\mathbf{P}_x, \mathbf{P}_j)$; $j = 1, 2, \dots, n$ is selected and transformed, by means of the corresponding normalization function $n^P(s^P)$, into palm-similarity measure N^P . Analogously, the minimum distance of $s^F(\mathbf{F}_x, \mathbf{F}_j)$; $j = 1, 2, \dots, n$ is selected and transformed into the face-similarity measure N^F . The final matching score, expressed as the total-similarity measure (TSM), is calculated using a simple sum fusion rule:

$$TSM = N^P + N^F. \quad (7)$$

The final decision about whether to accept or reject a user is made by comparing the TSM with the verification threshold T . If $TSM > T$, the user is accepted; otherwise, he/she is rejected.

3. Performance Evaluation

To evaluate the performance of the system a database containing palm and face samples was required. The XM2VTS frontal-face-image database was used as the face database (Messer *et al.*, 1999). We collected the hand database ourselves using a scanner. The spatial resolution of the palmar images is 180 dots per inch (dpi) / 256 grey levels. As the hand and the face databases contain samples belonging to different people, a ‘‘chimerical’’ multimodal database was created using pairs of artificially paired palm and face samples. Some examples of so paired palm and face samples from the database are presented in the Fig. 10.

The database was divided into two mutually exclusive sets: the training set and the testing set. The training set consisted of 440 image pairs of 110 people (4 image pairs per person) and was used as a training database for individual modalities and to get the distributions of the unimodal matching scores used in the decision fusion module.

The testing dataset consisted of 1048 image pairs of 131 people (8 image pairs per person) and was used exclusively for the evaluation of the system performance. Out of 8 image pairs for each person, 5 were used in the enrolment stage and 3 were used for testing. The tests involved trying to verify every test pair for every one of the 131 people enrolled in the database. This setup makes for 393 (131×3) valid-client experiments and 51090 ($131 \times 3 \times 130$) impostor experiments.

The results of the experiments, expressed in the terms of FRR (false rejection rate) and FAR (false acceptance rate), vary depending on the selected verification threshold T .



Fig. 10. Examples of the paired palmprint and face samples from our database.

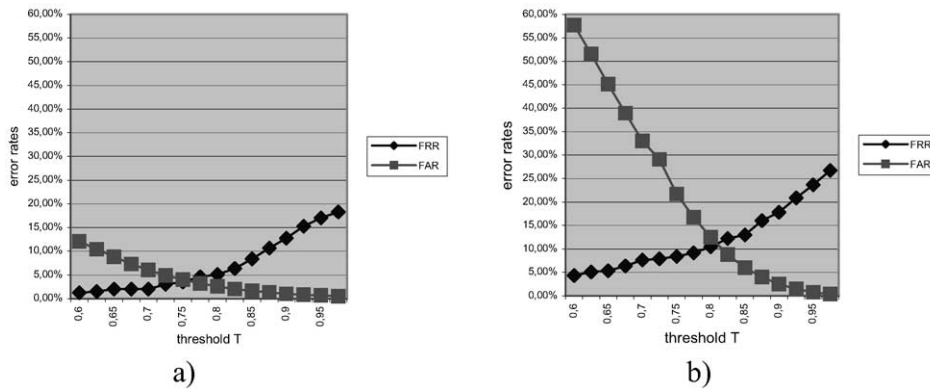


Fig. 11. Unimodal verification results, expressed as FRR and FAR depending on threshold T , obtained using a) palmprint modality, b) facial modality.

We first evaluated the unimodal performance of the system. When testing the unimodal system performance, the decision threshold T was related to the normalized similarity measures N^P or N^F , for the palmprint and face modality, respectively. The obtained results are presented in Fig. 11 a) for the palmprint modality and Fig. 11 b) for the face modality. From the results it is clear that the verification based on the palmprint easily outperforms the verification based on the face. The palmprint modality produces an EER (equal error rate) of 3.82% for $T = 0.755$, while the face modality produces an EER of 10.87% for $T = 0.81$. The minimum TER (total error rate) obtained using the palmprint features is 7.66% with $T = 0.8$, while the minimum TER obtained using the facial features is 18.97% with $T = 0.85$. The results are not surprising because it is already well known that systems based on palmprint features (Zhang *et al.*, 2003) produce better results than those based on facial features (Jonsson *et al.*, 1999).

Combining both modalities with fusion at the matching-score level as described in Subsection 2.4 and using different normalization techniques gives the error rates shown in Table 1. As can be seen from the Table 1, the best performance in terms of both EER and minimum TER is achieved using Bayes-based normalization.

Fig. 12 shows FAR and FRR for the bimodal system using Bayes-based normalization depending on the threshold T .

There, it can be seen that the fusion of palmprint and facial features improves the verification score, both by reducing the EER from 3.82% to 2.26% (for $T = 0.34$) and

Table 1
Error rates obtained on bimodal system by using different normalization techniques

	Piecewise-linear	min-max	median-MAD	double-sigmoid	tanh	z-score	Bayes
EER	2.79%	3.12%	2.79%	3.81%	3.05%	3.15%	2.29%
minTER	5.15%	6.39%	5.42%	5.72%	5.74%	5.56%	4.33%

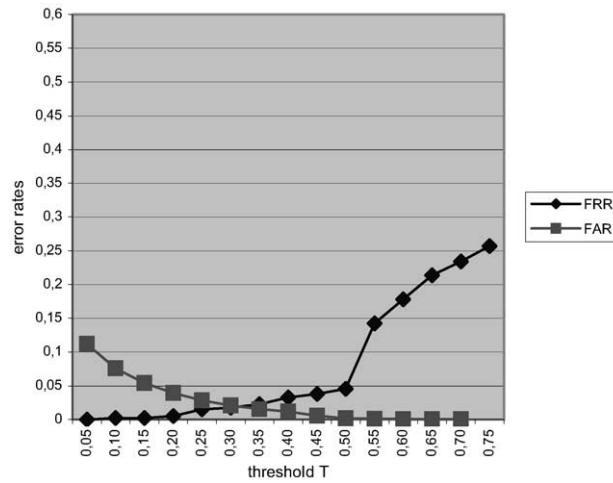


Fig. 12. The verification results using the bimodal system depending on threshold.

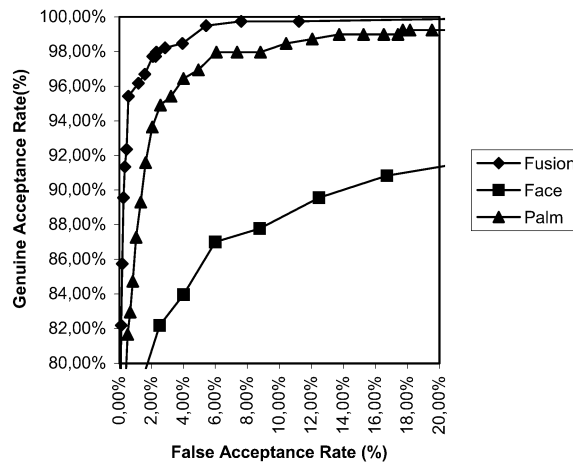


Fig. 13. Comparison of verification results for two unimodal systems and the bimodal system.

by reducing the minimum TER from 7.66% to 4.33% (for $T = 0.34$). The comparison of all three systems (two unimodal systems and a bimodal system) is given in Fig. 13.

In cases when two unimodal systems' performances are almost similar, it is expected that the fusion will give great improvements in performance. It has been experimentally demonstrated for various modalities (Kittler and Alkoot, 2003; Pavesic *et al.*, 2006). Some theoretical discussions on this can be found in (Kittler and Alkoot, 2003), although to prove such a claim we would need to assume the distribution of individual modalities matching scores as well as their independence.

For the proposed multimodal biometric system, a single-shot acquisition of image containing both face and palmprint could be applied and this leaves, in future, a plenty

of space to explore the fusion at the different levels. Such type of acquisition performed by one sensor, together with more sophisticated methods of image preprocessing and segmentation, feature extraction and followed by a fusion, would enable the development of unsupervised, touchless and robust on-line biometric verification system. Of course, the performance of such a system depends on quality of the input images, but we believe that owing to sophisticated methods of image processing and fusion at different levels the performance of such system can overtake the system described in the paper.

4. Conclusion

We have developed a bimodal biometric verification system based on the fusion of palmprint and facial features. A new approach for principal and other prominent palm lines recognition based on hypotheses generation and evaluation was proposed. The hypothesis collection consists of all palm line pairs (one line from live-template, one line from database template), which could correspond one to another based on two criteria: absolute angular difference between line orientations and their Euclidean distances. In the hypotheses evaluation phase a similarity measure is computed using all line segments of the palm lines in hypothesis. The palm line features were selected because they can be derived from images with low quality (Zhang and Shu, 1999), which can be important for touchless and single-shot acquisition of image containing both face and palmprint. This type of acquisition (performed by a camera), together with more sophisticated methods of preprocessing and segmentation, enables the development of robust on-line biometric system.

The experiments with different matching-score normalization techniques have been performed and the Bayes-based normalization was selected as the best-performing one.

The experimental results show that although palmprint-based unimodal systems significantly outperform face-based unimodal systems, fusion at the matching-score level can still be used to significantly improve the performance of the system.

The other reasons for including the face modality in biometric systems could be in the system usage for physical or logical access where the additional subsystem can log the facial images of the people accessing the secure object. The psychological effects of such multimodal system should also not be disregarded; it is likely that a system using multiple modalities would seem harder to cheat to any potential impostors.

In the future, we plan to concentrate on developing methods for robust palm and face feature extraction, including the features such as skin colour, from single-shot camera images. We also plan to include aliveness detection module to increase the robustness to fraudulent technologies.

References

- Ayache, N., and O.D. Faugeras (1986). A new approach for the recognition and positioning of two-dimensional objects. *IEEE Trans. Pattern Anal. Machine Intell.*, **8**, 44–54.

- Belhumeur, P., J. Hespanha and D. Kriegman (1997). Eigenfaces vs. fisherfaces: recognition using class specific linear projection. *IEEE Trans. Pattern Anal. and Machine Intell.*, **9**, 711–720.
- Bolle, R.M., J.H. Connel, S. Pankanti, N.K. Ratha and A.W. Senior (2004). *Guide to Biometrics*. Springer-Verlag, New York, Berlin, Heidelberg.
- Duda, R.O., P.E. Hart and D.G. Stork (2001). *Pattern Classification*. Wiley, New York.
- Duta, N., A.K. Jain and K.V. Mardia (2001). Matching of palmprints. *Pattern Recognition Lett.*, **23**, 477–485.
- Gonzales, R.C., and R.E. Woods (1993). *Digital Image Processing*. Addison Wesley, New York.
- Han, C.C., H.L. Cheng, K.C. Fan and C.L. Lin (2003). Personal authentication using palm-print features. *Pattern Recognition*, **36**, 371–381.
- Hough, P. (1962). *Methods and Means for Recognizing Complex Patterns*. US Patent 3069654.
- Jain, A.K., R. Bolle and S. Pankanti (Eds.) (1999a). *Biometrics: Personal Identification in Networked Society*. Kluwer Academic Publishers, USA.
- Jain, L.C., U. Halici, I. Hayashi and S.B. Lee (Eds.) (1999b). *Intelligent Biometric Techniques in Fingerprint and Face Recognition*. CRC Press.
- Jain, A.K., L. Hong and Y. Kulkarni (1999c). A multimodal biometric system using fingerprint, face and speech. In *Proc. 2nd Internat. Conf. on AVBPA*. pp. 182–187.
- Jain, A.K., and A. Ross (2002). Learning user-specific parameters in a multibiometric system. In *Proc. Internat. Conf. on Image Processing (ICIP)*. pp. 57–60.
- Jain, A.K., and A. Ross (2004). Multibiometric systems. *Communications of the ACM*, **47**, 34–40.
- Jain, A.K., K. Nandakumar and A. Ross (2005). Score normalization in multimodal biometric systems. *Pattern Recognition*, **38**, 2270–2285.
- Jones, M.J., and J.M. Rehg (1999). Statistical color models with application to skin detection. In *Proc. IEEE Conf. on Computer Vision and Pattern Recognition*. pp. 274–280.
- Jonsson, K., J. Kittler, Y.P. Li and J. Matas (1999). Support vector machines for face authentication. In *Proc. of British Machine Vision Conference BMVC99*. pp. 543–552.
- Kittler, J., and F.M. Alkoot (2003). Sum versus vote fusion in multiple classifier systems. *IEEE Trans. on Pattern Anal. and Machine Intell.*, **25**, 110–115.
- Kotropoulos, C., A. Tefas and I. Pitas (2000). Frontal face authentication using morphological elastic graph matching. *IEEE Trans. on Image Processing*, **9**, 555–560.
- Kumar, A., D.C.M. Wong, H.C. Shen and A.K. Jain (2003). Personal verification using palmprint and hand geometry biometric. In *Proc. 4th Internat. Conf. on Audio- and Video-Based Biometric Person Authentication (AVBPA)*. pp. 668–678.
- Kumar, A., and D. Zhang (2003). Integrating palmprint and face for user authentication. In *Proc. Multi Modal User Authentication Workshop*. Santa Barbara, CA, USA, Dec. 11–12. pp. 107–112.
- Li, W., D. Zhang and Z. Xu (2002). Palmprint identification by Fourier transform. *Int'l Journal of Pattern Recognition and Artificial Intelligence*, **16**, 417–432.
- Lu, G., D. Zhang and K. Wang (2003). Palmprint recognition using eigenpalms features. *Pattern Recognition Lett.*, **24**, 1463–1467.
- Maio, D., and D. Maltoni (1999). Minutiae extraction and filtering from grey-scale images. In L.C. Jain, U. Halici, I. Hayashi and S.B. Lee (Eds.), *Intelligent Biometric Techniques in Fingerprint and Face Recognition*. CRC Press. pp. 155–192.
- Messer, K., J. Matas, J. Kittler, J. Luetin and G. Maitre (1999). XM2VTSDB: the extended M2VTS database. In *2nd Internat. Conf. on Audio- and Video-based Biometric Person Authentication (AVBPA'99)*. Washington D.C. pp. 72–77.
- Navarrete, P., and J. Ruiz-Del-Solar (2002). Analysis and comparison of eigenspace-based face recognition approaches. *Int'l Journal of Pattern Recognition and Artificial Intelligence*, **16**, 817–830.
- Pavešić, N., I. Fratrić and S. Ribarić (2004). Degradation of the XM2VTS database face images. In *Proc. 2nd COST 275 Workshop, Biometrics on the Internet: Fundamentals, Advances and Applications*. Vigo, Spain. pp. 15–19.
- Pavesic, N., T. Savic and S. Ribaric (2006). Multimodal biometric authentication system based on hand features. In *From Data and Information Analysis to Knowledge Engineering*. Springer. pp. 630–637.
- Ribarić, S., D. Ribarić and N. Pavešić (2003). Multimodal biometric user-identification system for network-based applications. In *IEE Proc. Vision, Image & Signal Processing*, Vol. 150. pp. 409–416.
- Ribaric, S., and I. Fratric (2006). Experimental evaluation of matching-score normalization techniques on different multimodal biometric systems. In *Proc. 13th IEEE Mediterranean Electrotechnical Conf.* Malaga,

- Spain. pp. 498–501.
- Ribaric, S., I. Fratric and K. Kis (2005). A biometric verification system based on fusion of palmprint and face features. In *Proc. 4th Int'l Symposium on Image and Signal Processing and Analysis, ISPA 2005*. Zagreb. pp. 12–17.
- Ross, A., and A.K. Jain (2003). Information fusion in biometrics. *Pattern Recognition Lett.*, **24**, 2115–2125.
- Shu, W., and D. Zhang (1998). Automated personal identification by palmprint. *Optical Engineering*, **37**, 2359–2362.
- Turk, M., and A. Pentland (1991). Eigenfaces for recognition. *Journal of Cognitive Neuroscience*, **3**, 71–86.
- Wu, X., D. Zhang and K. Wang (2003). Fisherpalms based palmprint recognition. *Pattern Recognition Lett.*, **24**, 2829–2838.
- Wu, X., D. Zhang, K. Wang and B. Huang (2004). Palmprint classification using principal lines. *Pattern Recognition*, **37**, 1987–1998.
- You, J., W. Li and D. Zhang (2002). Hierarchical palmprint identification via multiple feature extraction. *Pattern Recognition*, **35**, 847–859.
- Zhang, D., and W. Shu (1999). Two novel characteristics in palmprint verification: datum point invariance and line feature matching. *Pattern Recognition*, **32**, 691–702.
- Zhang, D. (2000). *Automated Biometrics: Technologies & Systems*. Kluwer Academic Publishers, USA.
- Zhang, D., W.K. Kong, J. You and M. Wong (2003). Online palmprint identification. *IEEE Trans. Pattern Anal. and Machine Intell.*, **25**, 1041–1050.
- Zhao, W.Y., R. Chellappa, A. Rosenfeld and P.J. Phillips (2000). Face Recognition: A Literature Survey. *UMD CfAR Technical Report CAR-TR-948*.

S. Ribarić received the BS degree in electronics, the MS degree in automatics, and the PhD degree in electrical engineering from the Faculty of Electrical Engineering, Ljubljana, Slovenia, in 1974, 1976, and 1982, respectively. He is currently a full professor at the Department of Electronics, Microelectronics, Computer and Intelligent Systems, Faculty of Electrical Engineering and Computing, University of Zagreb, Croatia. His research interests include pattern recognition, artificial intelligence, biometrics, computer architecture and robot vision. He is author of more than 150 papers and four books (*Microprocessor Architecture*, *The Fifth Computer Generation Architecture*, *Advanced Microprocessor Architectures*, *CISC and RISC Computer Architecture*) and co-author of one (*An Introduction to Pattern Recognition*). Dr. Ribarić is a member of the IEEE, ISAI and IAPR.

I. Fratrić received his BS degree in computing from the University of Zagreb in 2003. He is currently a PhD student at the Department of Electronics, Microelectronics, Computer and Intelligent Systems at the Faculty of Electrical Engineering and Computing at the same university. His research interests include machine vision, pattern recognition, biometrics and artificial intelligence.

K. Kiš received her BS degree in computing from the University of Zagreb in 2003. She is currently a MS student at the Department of Electronics, Microelectronics, Computer and Intelligent Systems at the Faculty of Electrical Engineering and Computing at the same university.

Nauja biometrinė kombinuota delno antspaudų ir veido atpažinimu pagrįsta verifikavimo sistema

Slobodan RIBARIĆ, Ivan FRATRIĆ, Kristina KIŠ

Straipsnyje siūloma dvimodalė biometrinė verifikavimo sistema, apjungianti delno antspaudų ir veido savybių atitikimo įvertinimą. Sistema apjungia naują hipotezių generavimą ir įvertinimą pagrįstą delno esminių linijų atpažinimo ir gerai žinomą tikrinių veidų būdus. Skirtingų normalizavimo būdų tyrimai buvo atlikti siekiant pagerinti apjungimą atitikimo įvertinimo metu. "Chimerinė" duomenų bazė iš 241 asmens 1488 delno antspaudų ir veidų porų buvo naudojama sistemos projektavimui (110 asmenų 440 porų) ir testavimui (131 asmens 1048 poros). Tyrimo rezultatai rodo, kad sistemos pajėgumas yra ženkliai pagerintas lyginant su vienmodaliomis sistemomis.